Determination of Distilled Water Dielectric Constant by 2D-FDTD Method at X-Band Frequencies

1st Omaima Talmoudi
INPT
Rabat, Morocco
omaimatalmoudi@gmail.com

2th Lahcen Ait Benali
CPA-CRMEF CS
Casablanca, Morocco
aitbenalilahcen@hotmail.fr

3th Jaouad Terhzaz
CRMEF CS
Casablanca, Morocco
terhzazj@yahoo.fr

4th Abdelwahed Tribak
INPT
Rabat, Morocco
tribak_ma@yahoo.fr

5th Tomas Fernandez Ibañez
Universidad de Cantabria
Santander, Spain
tomas.fernandez@unican.es

***Abstract*—This paper presents a new iterative method for estimating the dielectric constant of distilled water using a WR90 shorted rectangular waveguide in the X-band with a hole that facilitates the insertion of water into the waterproof waveguide. The S11 parameter at the reference plane as a function of the dielectric constant of each layer is calculated by applying the two-dimensional finite-difference time-domain (2DFDTD) method to the wave equation. The Nelder-Mead algorithm is then applied to estimate the dielectric constant. This is done by comparing the results of S11 parameters. This method has been validated on two cases of monolayer and bilayer, such as air and air-plexiglass and plexiglass-distilled water.**

***Index Terms*—Characterization, S-parameters, microwave, waveguide, liquid material, dielectric constant.**

I. Introduction

Microwave liquid dielectric characterization is a vital area of study that focuses on understanding the behavior of liquid materials when exposed to microwave frequencies. In various applications, the dielectric properties of liquids become crucial factors, influencing the efficiency and performance of electronic devices. Characterization involves the measurement of parameters such as permittivity and loss tangent, which describe how a material responds to the electric field and dissipates energy, respectively[1][2].

One fundamental aspect of microwave liquid dielectric characterization is the use of specialized techniques and apparatus, such as rectangular waveguides. These waveguides provide a controlled environment for exposing liquid samples to microwave radiation, enabling researchers to investigate the material's response in a systematic* manner. By carefully analyzing the changes in electromagnetic wave propagation within the liquid, researchers can extract valuable information about its dielectric constants. This knowledge is particularly relevant in fields like material science, where the composition and behavior of liquids influence the design and performance of various materials[3][4].

The characterization process is crucial for optimizing the design of microwave devices and systems. For instance, in microwave heating applications, such as microwave ovens, an understanding of the dielectric properties of liquid foods ensures efficient energy absorption, leading to effective and uniform heating. In the telecommunications industry, liquid dielectric materials are employed in the construction of waveguides and resonators, allowing the controlled transmission and manipulation of microwaves[5]. Moreover, advancements in biomedical research benefit from microwave liquid dielectric characterization. The analysis of biological samples and liquids is essential for medical imaging technologies, where the dielectric properties of tissues play a vital role in generating accurate images. In summary, the comprehensive study of microwave liquid dielectric characterization not only enhances our understanding of fundamental electromagnetic interactions but also contributes to the development of innovative technologies across a wide range of applications[6][7][8]. Among the characterization methods, that based on rectangular waveguides stands out for its ability to characterize materials over a wide range of frequencies. However, these methods face challenges related to water and liquid tightness [15].The objective of our work is to develop a new method which will make it possible to resolve the sealing problem in the rectangular waveguide with a view to using it to characterize, initially distilled water in the X band .

II. Theory

A. Direct Problem

In this section, the calculation of the S11 parameter at the reference plane in the rectangular waveguide loaded by a bi-layer material as a function of the dielectric constant of each layer is shown in Fig. 1.

The bi-layer dielectric material consists of two layers, the first layer has a dielectric constant ε_1 and located between

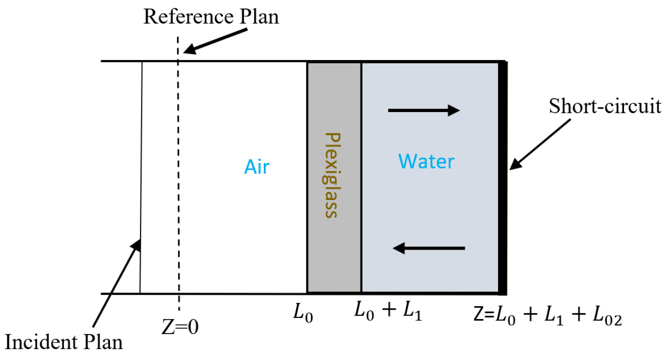

Fig. 1. Short-circuited rectangular waveguide loaded with a bi-layer dielectric material.

transverse planes $z = L_0$ and $z = L_0 + L_1$, the second layer has a dielectric constant ε_2 and is located between transverse planes $z = L0 + L1$ and $z = L0 + L1 + L2$. The waveguide is assumed to be excited by a dominant $TE10$ mode.

The electric field inside the rectangular waveguide is calculated using the wave equation 2D-FDTD method. The 2D-FDTD formulation is based on the direct discretization of the wave equation:

$$\frac{\partial^2 E_y}{\partial t^2} = \frac{1}{\varepsilon\ \mu}\left(\frac{\partial^2 E_y}{\partial x^2} + \frac{\partial^2 E_y}{\partial z^2}\right) \qquad (1)$$

Where ε and μ represent the dielectric constant and the permeability, respectively. We obtain the two-dimensional FDTD formulation for the component E_y of Equation 1 in Cartesian coordinates and following Yee's notation[9]:

$$E^{n+1}_{(i,k)} = 2E^{n}_{(i,k)} - E^{n-1}_{(i,k)} + \frac{c^2\Delta t^2}{\varepsilon_r\ (i,k)}\left[\frac{E^{n}_{(i+1,k)} + E^{n}_{(i-1,k)} - 2E^{n}_{(i,k)}}{\Delta x^2} + \frac{E^{n}_{(i,k+1)} + E^{n}_{(i,k-1)} - 2E^{n}_{(i,k)}}{\Delta z^2}\right] \qquad (2)$$

Here ε_1 is the dielectric constant and $\mu_r = 1$ is the relative permeability. Δx and Δz are the spatial steps along the two directions x and z, respectively, and Δt is the time step. To ensure the accuracy of the derivative space implied in the calculation of the electric field component, the mesh sizes of the FDTD network must be chosen to be sufficiently small compared to the wavelength [10][11].

$$\mathrm{Max}(\Delta x, \Delta z) < \frac{\lambda_{gmin}}{m_0} \qquad (3)$$

where $10 < m_0 < 100$ and $\lambda_g min$ is the minimum wavelength in the rectangular waveguide. For numeric stability of the 2D-FDTD algorithm, the increments Δt, Δx, and Δz must satisfy this stability condition [10][11]:

$$\Delta t \leq \frac{1}{c}\frac{1}{\sqrt{\frac{1}{\Delta x^2} + \frac{1}{\Delta z^2}}} \qquad (4)$$

Here, c denotes the speed of light in a vacuum. We need to place an absorbing boundary condition on the mesh to be truncated, using an artificial boundary that simulates the unlimited surroundings. The absorbing boundary in the z-direction is given by the following equation.

$$E^{n+1}_{(i,0)} = E^{n}_{(i,1)} + \frac{c\Delta t - \Delta z}{c\Delta t + \Delta z}[E^{n+1}_{(i,1)} - E^{n}_{(i,0)}] \qquad (5)$$

If the position of the absorbing boundary and the input waveguide is chosen such that only the fundamental mode can propagate, then the influence of higher-order modes in the input waveguide can be neglected.

The selected input port is then excited by its modal field distribution. A sinusoidally modulated Gaussian pulse is used to calculate the reflection coefficient:

$$E(x, z_s, t) = e^{-\left(\frac{t-t_0}{\tau}\right)^2} \sin(\omega_0 t)\sin\left(\frac{\pi x}{a}\right) \ (6)$$

After a suitable number of iterations, nt, a stable distribution is obtained and the DFT algorithm can be applied to obtain the desired complex field amplitude coefficient at the corresponding frequency.

The parameter $S11$ for the TE_10 mode is obtained by following the method described in [13]. The magnitude and phase of the mode amplitudes A and B are determined by applying the equations:

$$\int_0^a E(x, z_1)\sin\left(\frac{\pi x}{a}\right)dx = w_1 = A(z_1) + B(z_1) \qquad (7)$$

$$\int_0^a E(x, z_1 + \Delta z)\sin\left(\frac{\pi x}{a}\right)dx = w_2 = A(z_1)e^{-j\gamma\Delta z} + B(z_1)e^{+j\gamma\Delta z} \qquad (8)$$

Where $\sin\frac{x\pi}{a}$ is the normalized modal magnetic field and $\gamma = \sqrt{\frac{\omega[2]}{c[2]} - \frac{\pi[2]}{a[2]}}$ is the modal propagation constant. It gives:

$$S_{11} = \frac{B(z_1)}{A(z_1)} = \frac{w_2 - w_1 e^{-j\gamma\Delta z}}{w_1 e^{j\gamma\Delta z} + w_2} \qquad (9)$$

B. Inverse Problem

This section presents the calculation of the constant dielectric of the distilled water which fills the part of the rectangular waveguide WR90 between the plexiglass material and the short circuit (figure 1).

For this purpose, we use the optimization function $Fmin$ implemented in Python [14]. This function Fmin is based on the sequential simplex algorithm of NelderMead [12] and it solves nonlinear unconstrained multi-variable optimization problems that find the minimum of a scalar function of several variables, starting from an initial guess of the dielectric constant such as ε= 1.5. The error function minimized is the square sum of the differences between the measured and calculated $S11$ parameter, written as the following [15, 16]:

$$f(\varepsilon_{r1}, \tan\delta_1, \varepsilon_{r2}, \tan\delta_2) = abs(S_{11c} - S_{11m}) \qquad (10)$$

III. Numerical Result

To characterize distilled water using a short-circuited rectangular waveguide, it is necessary to place a solid dielectric material at the transverse plane of the latter to solve the sealing problem. In addition, a hole must be added to the longitudinal plane to facilitate the insertion of distilled water inside the waveguide as shown in Fig. 2.

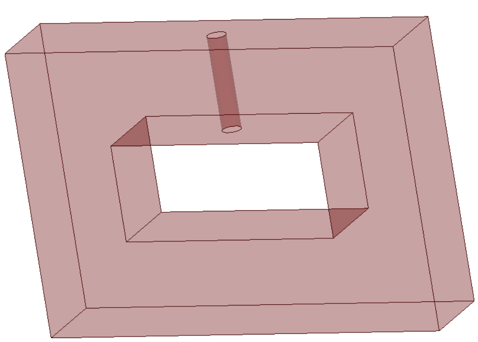

Fig. 2. View of rectangular waveguide WR90 with a hole on one side

The HFSS simulator is used to analyze and compare the electromagnetic behavior of the original WR90 waveguide without modification and the modified version with the introduced hole. Fig. 3 shows the result of the S11 parameter of the two structures.

It is interesting to note that the results show a general agreement between the two configurations. So, with this comparative analysis, we can see that the hole hasn't affected the performance of the waveguide.

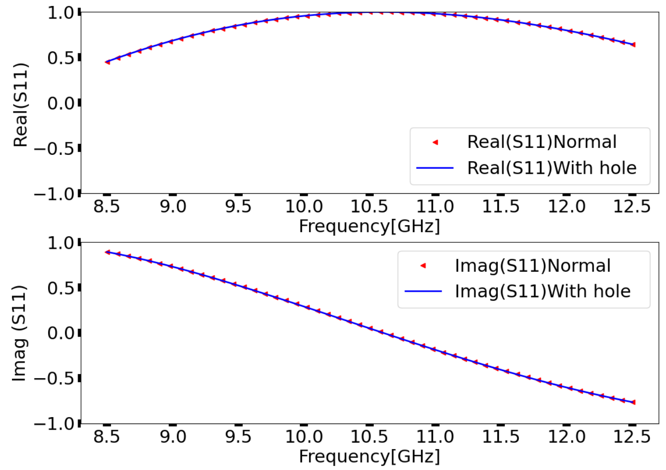

Fig. 3. S11 Parameter Analysis in HFSS: Comparing Short-Circuited Rectangular Waveguide WR90 in its Normal State with a WR90 Waveguide Featuring a Side Hole

With these results, we have decided to use the WR90 waveguide with a hole in all subsequent simulations. The results of the analysis we have carried out have demonstrated the viability of the WR90 waveguide with hole for our purposes and have provided the confidence to use it consistently in ongoing research and analysis.

A. direct Problem

For the validation of the direct problem, The reflection coefficient S11 as a function of frequency at the reference plane of the empty waveguide is shown in Fig.4 . It has been calculated using the FDTD method and compared with the reflection coefficient obtained using the HFSS simulator. The results of the FDTD and HFSS simulations are in very good agreement.

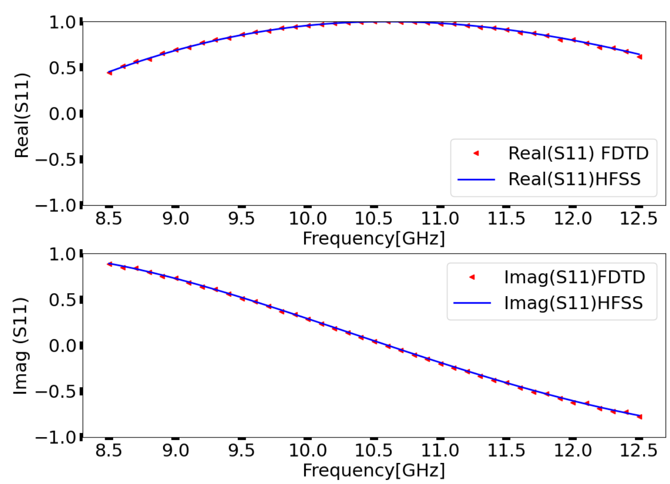

Fig. 4. $S11$ Parameter using FDTD in a short-circuited rectangular waveguide WR90 Empty, Compared with HFSS results

To validate the direct problem, the $S11$ parameter is calculated at the reference planes of the X-band rectangular

waveguide loaded with a monolayer dielectric Plexiglas (ε= 3.4) using the procedure described in Sec. II.A, also simulated with HFSS software as shown in Fig. 5.
These results show that there is an excellent agreement between the calculated and simulated S11 parameters.

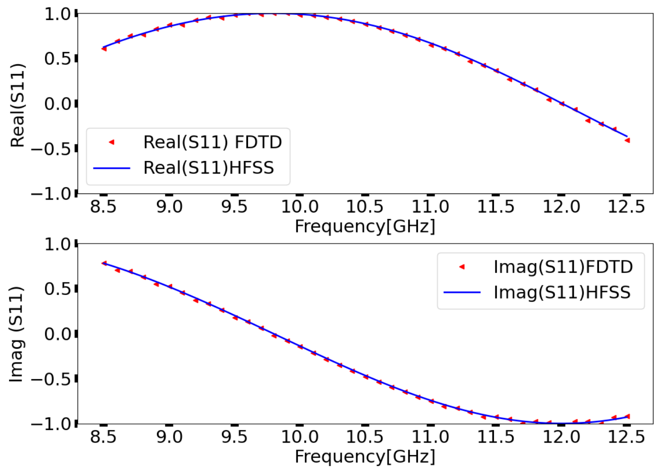

Fig. 5. $S11$ Parameter using FDTD in a short-circuited rectangular waveguide WR90 loaded by Plexiglass with thickness $3mm$, Compared with HFSS results

Then, the direct problem of the two-layer dielectric material is validated and the S11 parameters of a rectangular waveguide in the X-band loaded by a two-layer dielectric material consisting of Plexiglas (ε1= 3.4) with thickness $L1 = 3mm$ and distilled water (ε2= 61) with thickness$L2 = 4mm$ are obtained using the procedure described in Sec. II.A and simulated by using HFSS software. There is good agreement between the calculated and simulated S11 parameters as shown in Fig. 6.

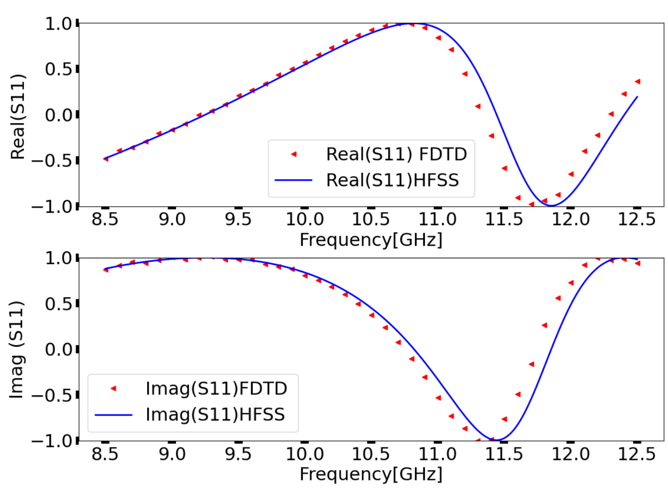

Fig. 6. $S11$ Parameter using FDTD in a short-circuited rectangular waveguide WR90 loaded by bilayer Plexiglass and distilled water, Compared with HFSS results

B. Inverse Problem

For the inverse problem, the dielectric constant of a monolayer dielectric material and each layer of a bilayer dielectric material were determined in the X-band frequencies using the procedure described in Section II. The S11 parameters at the reference plane of a WR90 X-band rectangular waveguide loaded with a single or bilayer dielectric material were calculated.

1) Dielectric constant of monolayer:

We first used this method to estimate the dielectric constant of the monolayer dielectric material simulated at the X-band frequencies. The initial guess of the dielectric constant was ε1= 1.5. The dielectric constant values of Plexiglas of 3 mm thickness were determined. Fig. 7 shows the results obtained. The results obtained for the dielectric constant of monolayers

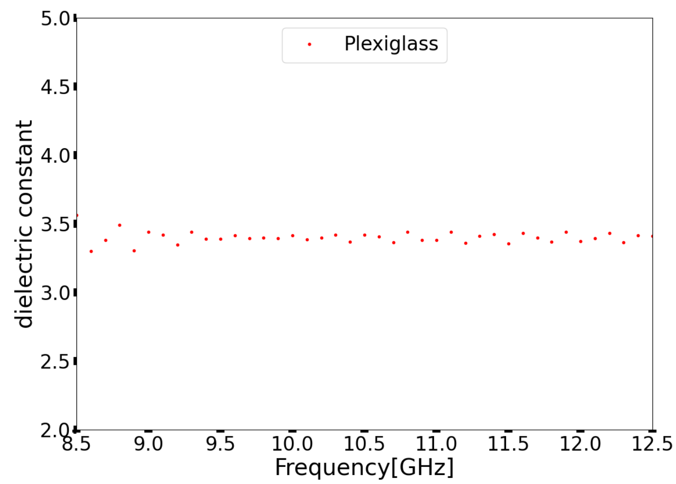

Fig. 7. The Dielectric Constant for a Monolayer of 3mm Plexiglass Using the Inverse Procedure with the Nelder-Mead Algorithm

using the procedure described in this Work agree well with

2) Dielectric constant of distilled water:

We have estimated the dielectric constant of the bilayer dielectric material plexiglass-water simulated at the X-band frequencies using this same procedure.

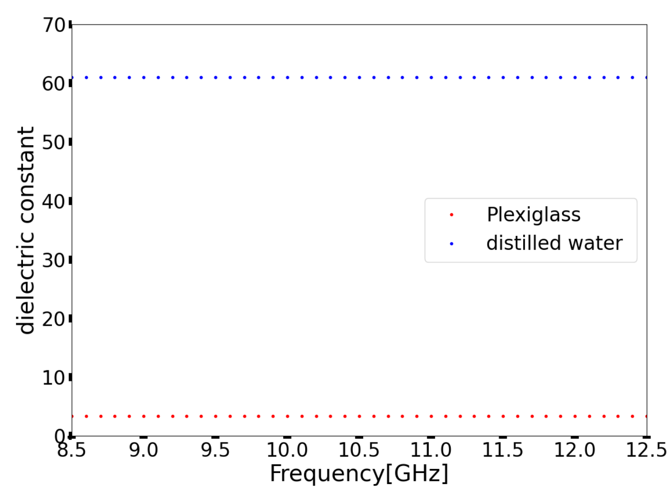

Fig. 8. The Dielectric Constants for a bilayer of 3mm Plexiglass and 4mm Distilled Water Using the Inverse Procedure with the Nelder-Mead Algorithm

The initial estimates of the dielectric constant of Plexiglas and distilled water were $\varepsilon 1$= 1.5 and $\varepsilon 2$= 10. The dielectric constant values of Plexiglas 3mm (thickness) and distilled water 4mm (thickness) were determined. The results obtained are shown in Fig. 8. The results of the dielectric constant of distilled water obtained by the method presented in this work are in good agreement with the results given in the literature.

IV. CONCLUSION

In this paper, a new method has been presented to estimate the dielectric constant of distilled water using a WR90 shorted rectangular waveguide in the X-band.

In particular, this waveguide is unique in its construction with a hole placed on one side. This novel design enhances the waveguide's ability to characterize liquid materials such as water. The 2D FDTD method is used to calculate the S11 parameters as a function of the dielectric constant of each layer. The Nelder-Mead algorithm was used to estimate the dielectric constant of each layer in a bilayer dielectric material by comparing the calculated value with the simulated value of the S11 parameters of an X-band rectangular waveguide loaded with a bilayer dielectric material. The results obtained are in good agreement and the method has been validated using bilayer dielectric materials such as Plexiglas and distilled water.

REFERENCES

[1] A. Javed, A. Arif, M. Zubair, M. Q. Mehmood, and K. Riaz, "A low-cost multiple complementary split-ring resonator-based microwave sensor for contactless dielectric characterization of liquids," IEEE Sens. J., vol. 20, no. 19, pp. 11326-11334, 2020.

[2] E. L. Chuma, Y. Iano, G. Fontgalland, and L. L. B. Roger, "Microwave sensor for liquid dielectric characterization based on metamaterial complementary split ring resonator," IEEE Sens. J., vol. 18, no. 24, pp. 9978-9983, 2018.

[3] W. Cha-um, P. Rattanadecho, and W. Pakdee, "Experimental and numerical analysis of microwave heating of water and oil using a rectangular waveguide: influence of sample sizes, positions, and microwave power," FOOD BIOPROCESS TECH, vol. 4, pp. 544-558, 2011.

[4] K. Gupta and P. S. Hall, "Analysis and Design of Integrated Circuit-Antenna Modules," Wiley, 1999.

[5] A. Soffiatti, Y. Max, S. G. Silva, and L. M. de Mendonça, "Microwave metamaterial-based sensor for dielectric characterization of liquids," Sensors, vol. 18, no. 5, p. 1513, 2018.

[6] M. S. Venkatesh and G. S. V. Raghavan, "An overview of dielectric properties measuring techniques," Can. Biosyst. Eng., vol. 47, no. 7, pp. 15-30, 2005.

[7] M. D. Deshpande and K. Dudley, "Estimation of complex permittivity of composite multilayer material at microwave frequency using waveguide measurements," (No. NAS 1.15: 212398), 2003.

[8] A. Ishimaru, Electromagnetic Wave Propagation, Radiation, and Scattering: From Fundamentals to Applications, John Wiley & Sons, 2017.

[9] D. V. Krupezevic, V. J. Brankovic, and F. Arndt, "The wave-equation FD-TD method for the efficient eigenvalue analysis and S-matrix computation of waveguide structures," IEEE Trans. Microw. Theory Tech., vol. 41, no. 12, pp. 2109-2115, 1993.

[10] U. C. Hasar, "Permittivity measurement of thin dielectric materials from reflection-only measurements using one-port vector network analyzers," Prog. Electromagn. Res., vol. 95, pp. 365-380, 2009.

[11] U. C. Hasar, "Unique Permittivity Determination of Low-loss Dielectric Materials from Transmission Measurements at Microwave Frequencies," PIER, vol. 107, July 2010.

[12] J. A. Nelder and R. Mead, "A simplex method for function minimization," Comput. J., vol. 7, no. 4, pp. 308-313, 1965.

[13] . Elmajid, J. Terhzaz, H. Ammor, M. Chaïbi, and Á. Mediavilla Sánchez, "A new method to determine the complex permittivity and complex permeability of dielectric materials at X-band frequencies," 2015.

[14] Optimization User's Guide, Python , Version 3.10.4, 2022.

[15] L. A. Benali, J. Terhzaz, A. Tribak, and A. M. Sanchez, "2D-FDTD method to estimate the complex permittivity of a multilayer dielectric materials at Ku-band frequencies," Prog. Electromagn. Res. M, vol. 91, pp. 155-164, 2020.

[16] L. Ait Benali, A. Tribak, J. Terhzaz, and T. F. Ibanez, "New FDTD Method to Estimate the Dielectric Constant and Loss Tangent of a Bilayer Dielectric Material at X-Band Frequencies," IJMOT , vol. 18, no. 6, 2023.